Proceedings of the 11th Brazilian Congress of Thermal Sciences and Engineering -- ENCIT 2006
Braz. Soc. of Mechanical Sciences and Engineering -- ABCM, Curitiba, Brazil,- Dec. 5-8, 2006

Paper CIT06-0444

MOISTURE TRANSPORT IN WOOD.
Material data, calculation model and comparison with measurements.

Jesper Arfvidsson
Dept. of Building Physics, Lund University, Box 118, 221 00 Lund, Sweden.
Jesper.arfvidsson@byggtek.lth.se

To predict the risk of mould growth, rot, deformations and cracks in wood, it is necessary to know the moisture levels in constructions and building components. This paper presents a theory and a two-dimensional PC-model based on the use of Kirchhoff potentials to calculate moisture flow in wood. Anisotropy is allowed for using different flow coefficients in the different directions, in both sapwood and heartwood. The theory also deals with the internal boundary between sapwood and heartwood, and the external boundary to the outer air. The discrete form of the partial differential equation and the numerical technique to solve the problem are presented. The values of the flow coefficients used in the model are based on direct laboratory measurements. Calculation results from the model are compared with independently measured two-dimensional moisture distributions. The agreement is good.
The choice of moisture flow potential has been a matter of controversy. Different potentials have been advocated as the best choice. It is shown that Kirchhoff's potential has advantages both in the mathematical and the numerical formulations, and in the experimental determination of moisture flow data.

Keywords*. moisture transport, wood, calculation model, Kirchhoff potential*

1. Introduction

Moisture transport in porous material is a complicated non-linear process that changes with moisture conditions. Different models to calculate the moisture flow have been developed during the past. One class of models does not consider the variable moisture distribution through the material. The average moisture content curve versus time is found from suitable combinations of analytical and empirical relations for the boundary flow under different conditions.

Another class of models is the ones based on partial differential equations, for example Luikow (1966). His equation system has been solved analytically with constant parameters (Liu, 1990) and numerically with variable parameters (Stanish et al 1984; Plumb et al 1984; Avramides et al 1992). The values for the different parameters and relations, for example the temperature dependence of moisture flow coefficients, are often obtained from a mixture between assumptions and measurements. Very often the results from the models are focused on the average moisture content.

To calculate stresses that cause deformations and cracks in a piece of wood during drying, it is necessary to know the *moisture distribution* during a process. A model for moisture distributions is much more sensitive to the internal flow processes than a model for the average, or total, drying with time. It is imperative to have good data for the internal moisture flow coefficients and in particular for their variation with the moisture state.

The moisture flow calculation in wood during drying is complicated considerably by the polar anisotropy. There are different moisture flow coefficients in radial, tangential and fibre directions for both heartwood and sapwood. These coefficients depend strongly on the moisture content, which causes interpolation difficulties in the numerical calculations. This interpolation problem may however be removed completely by the use of a Kirchhoff transformation. In the presented two-dimensional calculation model four different Kirchhoff potentials for the moisture flow are used to take care of the anisotropy of wood.

A main purpose of the present model is to predict the distributions of moisture content at different times during drying. We have endeavored to use as few assumptions as possible and to base the moisture flow calculations on data from direct measurements on sapwood and heartwood in all three directions. The approach is a phenomenological one, where ad hoc assumptions about flow on the fiber level are avoided.

A general Fickian approach is used. Fickian moisture flow is based on the use of a well-defined moisture state variable. The flow is proportional to the gradient of the moisture state variable, and the moisture flow coefficient depends on the moisture state. In a Fickian process, the moisture flow is determined by differences of the moisture state variable between adjacent layers. In the isothermal case with known relations between the moisture state variables, it does not really matter which potential we use. An exception is, in our opinion, the so-called Kirchhoff's flow potential, which has distinct advantages considering simplicity in both theory and numerical applications, (Arfvidsson and Claesson 1989).

Moisture flow due to temperature or total gas pressure gradients in the wood is not considered in the theory and model presented here. The temperature level may change with time.

2. Moisture State Variables

Any one of the following state variables may determine or characterize the local moisture state in any small part of humid wood: relative humidity φ, absolute humidity v or water vapour pressure p, pore water pressure $P_{p.w.}$, chemical potential μ_w for water, or moisture content u (kg/kg). Let ϕ denote *any* of these moisture state variables:

$$\phi = \varphi, v, p, P_{p.w.}, \mu_w \quad \text{or} \quad u \tag{1}$$

We consider the case of essentially constant total air pressure and spatially constant temperature. There are a number of relations between the moisture state variables. We have the gas law for vapour pressure, Kelvin's law for pore water pressure, $\ln(\varphi)$-dependence for the chemical potential, and the measured sorption isotherm. See for example Claesson (1997). The moisture state is then determined, when one of the above variables is known. The process is determined by a single moisture state variable ϕ. The temperature is constant throughout the drying wood specimen. The temperature level may change with time as long as the temperature distribution is kept uniform, without a significant temperature gradient in the material.

3. Fickian Moisture Flow

The moisture flow g (kg/m^{2}s) is in most models described by a Fickian flow law. In three dimensions we have:

$$\vec{g} = -D_\phi(\phi)\nabla\phi \quad \nabla\phi = \left(\frac{\partial\phi}{\partial x}, \frac{\partial\phi}{\partial y}, \frac{\partial\phi}{\partial z}\right) \tag{2}$$

The moisture flow coefficient D_ϕ depends on the moisture state ϕ (and on the temperature). The relation between the moisture flow coefficients D_ϕ and $D_{\phi'}$ for any two moisture state variables ϕ and ϕ' from Eq.(1) is:

$$D_\phi = D_{\phi'}\frac{d\phi'}{d\phi} \tag{3}$$

Here, the derivative of $\phi'(\phi)$ (for constant temperature) is involved. It is clear that the choice of flow potential does not matter when the functional relation $\phi' = \phi'(\phi)$ is known from the relations between the moisture state variables Eq.(1).

In numerical simulations, moisture flows between adjacent cells are calculated from Fick's law at each timestep. A particular problem is the variation of the flow coefficient D_ϕ with the moisture state ϕ. In a one-dimensional steady state case we have:

$$-g = D_\phi(\phi)\frac{d\phi}{dx} \tag{4}$$

This is an ordinary, non-linear differential equation. The flow g is independent of x. Integration over an interval from x_1 to x_2, or between two nodes in a numerical mesh, gives the exact solution:

$$(-g)\cdot(x_2 - x_1) = \int_{x_1}^{x_2} D_\phi(\phi(x'))\frac{d\phi}{dx'}dx' = \int_{\phi(x_1)}^{\phi(x_2)} D_\phi(\phi)d\phi \tag{5}$$

In many models a suitable average value for D_ϕ is used. The exact average is given by the above integral of D_ϕ. In numerical modeling of moisture transport, we have found that is much better to use this integrated form.

4. Kirchhoff's Flow Potential

In the three-dimensional isotropic case, the moisture flow is given by Eq.(2). The flow coefficient D_ϕ depends on ϕ. Kirchhoff originally introduced Kirchhoff's flow potential for heat conduction with temperature-dependent thermal conductivity (Carslaw & Jaeger, 1959). For state-dependent moisture flow, the corresponding potential is defined by:

$$\psi(\phi) = \psi_{ref} + \int_{\phi_{ref}}^{\phi} D_\phi(\phi)d\phi \tag{6}$$

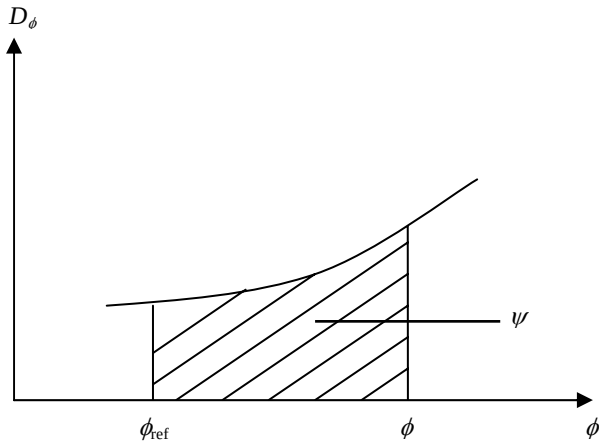

Figure 1. Kirchhoff's flow potential $\psi(\phi)$ which is the area under the curve $D_\phi(\phi)$, (6).

The potential ψ is the area under the curve $D_\phi(\phi)$ between ϕ_{ref} and ϕ, see Figure 1. It is a function of ϕ for each material: $\psi=\psi(\phi)$. It follows from Eq. (3) that the flow potential ψ is independent of which ϕ and D_ϕ one chooses to use. The reference values ϕ_{ref} and ψ_{ref} can be chosen arbitrarily for each material. We normally, by convenience, put the value of ψ to zero for the reference level ϕ_{ref} for the material: $\psi_{ref} = 0$. The derivative of $\psi(\phi)$ gives the flow coefficient D_ϕ. Using Eq. (3), the flow coefficient D_ψ becomes equal to 1:

$$\frac{d\psi}{d\phi} = D_\phi(\phi) \quad D_\psi = D_\phi \cdot \frac{d\phi}{d\psi} = 1 \tag{7}$$

The variable flow coefficient vanishes. The moisture flow has the following simple form without a state-dependent flow coefficient:

$$\vec{g} = -\nabla\psi \tag{8}$$

5. Moisture Balance Equation

The general moisture balance equation is:

$$\rho_d \frac{\partial u}{\partial t} = -\nabla \cdot \vec{g} \tag{9}$$

Here ρ_d is the dry density of the material.
Using the Kirchhoff's flow potential, the moisture balance equation has the following simple form, Eq.(8-9):

$$\rho_d \frac{\partial u}{\partial t} = \frac{\partial^2\psi}{\partial x^2} + \frac{\partial^2\psi}{\partial y^2} + \frac{\partial^2\psi}{\partial z^2} = \nabla^2\psi \tag{10}$$

This equation for the moisture flow process in an isotropic, homogeneous material involves only the moisture content u and Kirchhoff's moisture flow potential ψ. The functional relation between u and ψ is needed:

$$u = u(\psi) \tag{11}$$

In a conventional Fickian description, the moisture content is given by the measured sorption isotherm, $u=u(\varphi)$, and the moisture flow by a flow coefficient $D_\phi(\phi)$. The description involves two functions of the moisture state. From $D_\phi(\phi)$, we get $\psi(\phi)$, Eq.(6). The combination of $u(\phi)$ and $\psi(\phi)$ gives the relation $u(\psi)$. In our description, based on Kirchhoff's potential, we use the relation $u(\psi)$ internally. The sorption isotherm is needed at internal and external boundaries. See Fig. 2.

6. Determining ψ from Steady-state Measurements

Internally in the material we only need the relation $u=u(\psi)$. It is interesting to notice that this basic relation may be determined directly from a steady-state measurement.

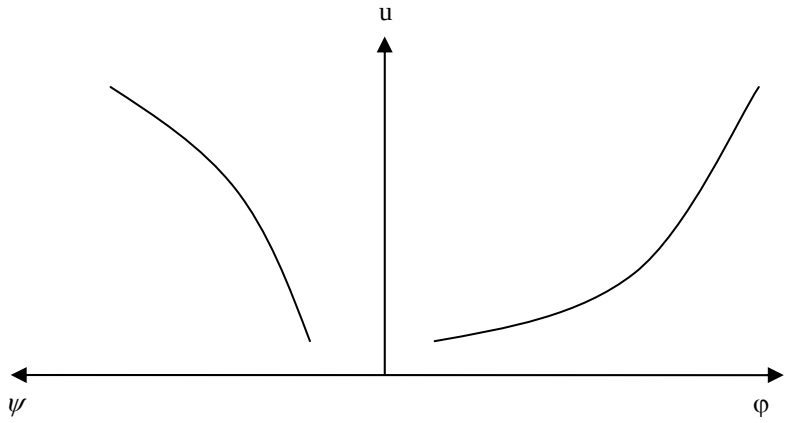

Figure 2. Representation of flow and sorption properties in two curves. The relation between u and ψ is used internally in the material, and the relation between u and φ at boundaries.

We consider a one-dimensional steady-state situation in a slab $0 \le x \le$ L. The reference state $u = u_{ref}$ is kept on one side, $x=0$, and $u = u_L$ is kept on the other side, $x=L$, Fig. 3. We have:

$$
\begin{aligned}
& -g = \frac{d\psi}{dx} \\
& -g \cdot (x-0) = \psi(x) - \psi(0) \\
& x = \frac{\psi}{-g}
\end{aligned}
\qquad (12)
$$

Kirchhoff's flow potential varies linearly with x through the slab. The potential ψ is obtained by multiplying x by the factor $(-g)$. Let $u(x)$ be the measured moisture content through the slab, Fig. 3. The relation between u and x gives the relation between u and ψ obtained by multiplying x by the factor $(-g)$.

By measuring $u(x)$ and the constant flow g, we obtain $u(\psi)$ directly. In a conventional evaluation, the flow coefficient $D_u(u)$ is obtained by $-g$ divided by the derivative du/dx. In an exact numerical calculation to determine the flow between nodes, we need to integrate $D_u(u)$ according to Eq.(5). This 'circular' procedure is avoided if ψ is used directly.

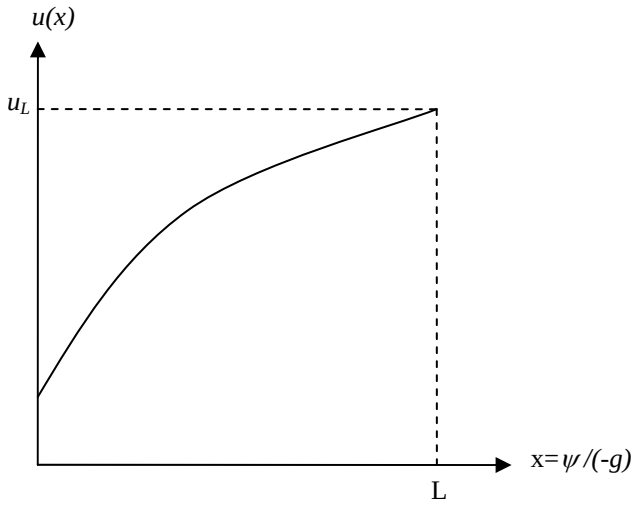

Fig 3. Steady-state distribution of moisture *u(x)* through a slab. The curve and the measured flow *g* give *u(ψ)* for the material, Eq.(12).

7. External Boundary

Let v_{air} be the absolute humidity of the air, and v_{surf} the absolute humidity at the surface (Figure 4). We use the following boundary condition:

$$g_n = -\left.\frac{\partial \psi}{\partial n}\right|_{surf} = \beta_v (v_{surf} - v_{air}) \tag{13}$$

Here, n denotes the normal coordinate (directed outwards), and β_v (m/s) is the surface moisture transfer coefficient related to a difference in *v*. It depends on the airflow conditions. There may be a moisture flow resistance between v_{surf} and the open-air surface. In this case the moisture flow over the boundary is lower and β_v is lower than values from the literature.

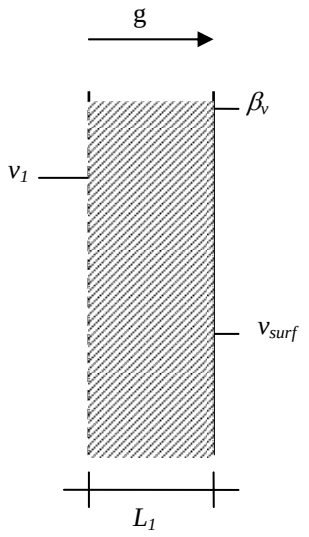

Fig. 4. Steady-state flow through a surface layer and a part L_1 of the wood.

The surface flow may be expressed in moisture content *u* instead. Then we have for the right-hand side of Eq.(13):

$$\beta_u (u_{surf} - u_{air}) = \beta_v (v_{surf} - v_{air}) \tag{14}$$

Here, $u_{air}=u(\varphi_{air})$ is the equilibrium moisture content for the relative humidity φ_{air} of the air. We expect the factor β_v to be fairly constant. Then β_u may vary considerably due to the relations $u_{surf}=u(\varphi_{surf})$, $\varphi_{surf}=v_{surf}/v_{sat}(T_{surf})$ and $u_{air}=u(\varphi_{air})$, $\varphi_{air}=v_{air}/v_{sat}(T_{air})$. There is a variation caused by the different temperatures in the vapour content at saturation, $v_{sat}(T)$, and by the sorption isotherm. Therefore, we avoid the formulation involving β_u and u.

Let us now consider the boundary condition between the outside air and a point at the depth L_1 inside the material, see Figure 4. The vapour content at this depth is v_1, which might be the value in the first internal node in a numerical model. We seek the flow g_n and the vapour content v_{surf} at the surface We use a constant value of β_v. Here, we use Kirchhoff's potential $\psi(v)$ with vapour content as dependent variable. We have in a local steady-state situation:

$$g_n = \frac{\psi(v_1)-\psi(v_{surf})}{L_1} = \beta_v (v_{surf} - v_{air}) \tag{15}$$

The equation to determine v_{surf} is then:

$$g_n = \psi(v_1)-\psi(v_{surf}) = L_1\beta_v (v_{surf} - v_{air}) \tag{16}$$

8. Anisotropy

Let r, θ, z be the cylindrical coordinates fitted to the sapwood-heartwood boundary. There are different moisture flow coefficients $D_r(\phi)$, $D_\theta(\phi)$, $D_z(\phi)$, in radial, tangential and axial or fibre direction:

$$-g = \hat{r}\cdot D_r(\phi)\frac{\partial\phi}{\partial r} + \hat{\theta}\cdot D_\theta(\phi)\frac{1}{r}\frac{\partial\phi}{\partial\theta} + \hat{z}\cdot D_z(\phi)\frac{\partial\phi}{\partial z} \tag{17}$$

Here $\hat{r}, \hat{\theta}$, and $\hat{z}$ are unit vectors in the three cylindrical directions.

The flow coefficients may be different in heartwood and in sapwood. We get in the general three-dimensional case *six flow coefficients*, which all are functions of the moisture state ϕ (and the temperature). For each flow coefficient we define a corresponding Kirchhoff potential:

$$\psi_\alpha^A = \psi_{ref} + \int_{\phi_{ref}}^{\phi} D_\alpha^A(\phi')d\phi' \tag{18}$$

A = sapwood or heartwood

$$\alpha = r, \theta, z$$

All six potentials are evaluated with the Kirchhoffian moment method (Rosenkilde and Arfvidsson, 1997).

The moisture flow vector Eq.(17) in heartwood and in sapwood becomes:

$$-\vec{g}^A = \hat{r}\cdot\frac{\partial\psi_r^A}{\partial r} + \hat{\theta}\cdot\frac{1}{r}\frac{\partial\psi_\theta^A}{\partial\theta} + \hat{z}\cdot\frac{\partial\psi_z^A}{\partial z} \tag{19}$$

This expression for the flow is inserted in the general moisture balance equation, Eq.(9). In cylindrical coordinates the moisture balance equation for wood becomes:

$$\rho_d\frac{\partial u}{\partial t} = \frac{1}{r}\frac{\partial}{\partial r}\left(r\frac{\partial\psi_r^A}{\partial r}\right) + \frac{1}{r^2}\frac{\partial^2\psi_\theta^A}{\partial\theta^2} + \frac{\partial^2\psi_z^A}{\partial z^2} \tag{20}$$

9. Internal Boundary

There is an internal boundary between heartwood and sapwood. Intensive variables (φ, v, p, $P_{p,w}$ and μ_w) are continuous at an internal boundary, while u is discontinuous. The flow coefficients, and in particular ψ, are of course different in different materials. We consider the boundary between sapwood and heartwood. The radial moisture flow-

coefficients are $D_{\phi,r}^{sap}(\phi)$ and $D_{\phi,r}^{heart}(\phi)$, and the corresponding Kirchhoff potential $\psi_r^{sap}(\phi)$ and $\psi_r^{heart}(\phi)$. The normal flow has to be continuous. We have the following boundary condition:

$$\frac{\partial \psi_r^{heart}}{\partial r} = \frac{\partial \psi_r^{sap}}{\partial r} \tag{21}$$

Figure 5 shows the one-dimensional steady-state case with an internal boundary between any two materials *A* and *B*. In our case we have $\psi_A = \psi_r^{heart}$ and $\psi_B = \psi_r^{sap}$. The values ϕ_1 and ϕ_2 are known, and the boundary value ϕ_{12} is to be determined. Here ϕ denotes any one of the variables in Eq.(1) except *u*. Using Kirchhoff potentials, we have:

$$g = \frac{\psi_A(\phi_1) - \psi_A(\phi_{12})}{L_A} = \frac{\psi_B(\phi_{12}) - \psi_B(\phi_2)}{L_B} \tag{22}$$

or

$$\psi_B(\phi_2) - \psi_B(\phi_{12}) = \frac{L_B}{L_A} \cdot \psi_A(\phi_{12}) - \frac{L_B}{L_A} \cdot \psi_A(\phi_1) \tag{23}$$

This equation determines ϕ_{12}.

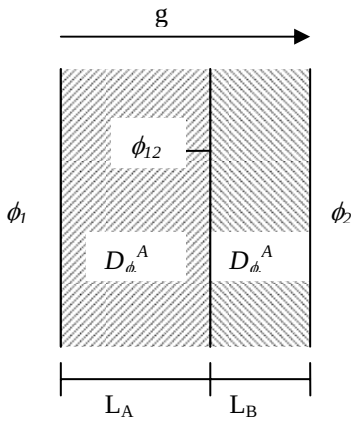

Figure 5. Steady-state flow through a slab consisting of two materials *A* and *B*.

10. Comparison with Experiments

10.1 Material data

Experimental results for Scots pine (*pinus silvestris*) are reported in Rosenkilde and Arfvidsson (1997). Moisture content distributions were measured in a number of specimens during a one-dimensional drying process. The specimens were dried from green condition in climate chamber at 60°C and 60% relative humidity. The specimens were made of heartwood and sapwood and sealed on four sides to establish a one-dimensional moisture flow either in radial, tangential or axial direction. Two different methods were used to measure the transient moisture distribution in the specimens. In the first method the specimen was cut into thin slices and the medium moisture content in each slice were evaluated using the dry weight method. This method worked well in tangential and radial directions. In the axial direction computer tomography (CT) scanning technology was used. This is a non-destructive method allowing measurements to be performed in the specimen during the whole drying period. The CT-scanner uses an X-ray tube and a detector array that rotates around the specimen. The method using CT-scanning to measure moisture distributions in wood is well described by Lindgren (1988, 1992).

The measured transient moisture distributions were then evaluated, using the evaluation method presented by Rosenkilde and Arfvidsson (1997). The obtained relations between *u* and ψ for radial, tangential and axial flow in heartwood and in sapwood at 60°C are shown in Table 1. In Rosenkilde and Arfvidsson, 1997, these results are presented as six curves. The corresponding curves using conventional moisture flow coefficients are also given.

Table 1. The Kirchhoff flow potential ψ at 60 ^{o}C for Scots pine sapwood and heartwood in all three directions to grain: radial, tangential and longitudinal

	Sapwood			Heartwood		
	long.	tan.	rad.	long.	tan.	rad
w kg/m^3	$\psi\cdot10^7$ kg/ms	$\psi\cdot10^7$ kg/ms	$\psi\cdot10^7$ kg/ms	$\psi\cdot10^7$ kg/ms	$\psi\cdot10^7$ kg/ms	$\psi\cdot10^7$ kg/ms
40	0.40					
50	0.70		0.13		0.13	0.15
60	1.1	0.10	0.18	0.15	0.19	0.20
70	1.4	0.18	0.25	0.40	0.25	0.26
80	1.8	0.26	0.35	0.70	0.33	0.33
90	2.1	0.36	0.45	1.0	0.41	0.40
100	2.5	0.46	0.60	1.3	0.50	0.48
110	2.9	0.60	0.78	1.6	0.60	0.58
120	3.2	0.73	1.1	2.0	0.69	0.67
130	3.6	0.85	1.4	2.3	0.78	0.79
140	4.0	1.0		2.7	0.90	0.93
145		1.0				
150	4.6			3.0	1.1	1.1
155					1.2	
160	5.6			3.3		
165	6.2					
170				3.6		

10.2 Test experiment

Samuelsson & Arfvidsson (1994) presented two-dimensional transient measurements on wood during drying. The specimens were made of Scots pine and contained both heartwood and sapwood. The specimens have the following dimensions: length 1200 mm, width 144 mm and thickness 50 mm. The average density (ρ_d) was 417kg/m^3. For the chosen specimen (No. 3) the heartwood percentage was 76% (Fig. 6). The specimens were dried in a experimental kiln, the first 72 hours at 52°C and 67% relative humidity, and then for 72 hours at 53,3°C and 52% relative humidity. Samples from the specimen were cut at different times during the drying. Each sample had a thickness of 31mm. The distance between the samples was 130mm. After each cut the crosscut was insulated with silicon to prevent axial moisture transport. The two-dimensional moisture distribution was measured using a cutting technique. Each sample was cut in 65 small rectangular pieces and the moisture content immediately measured using the dry weight method.

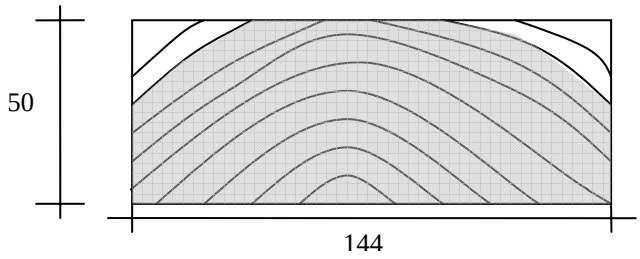

Figure 6. The test specimen used in the comparison between measurements and calculations. It is made of Scots pine with a length of 1200mm, a width of 144mm and a thickness of 50mm. The darker parts in the figure are heartwood.

10.3 Calculations

Calculations were made using a PC-program based on the described calculation model. The material data used in the calculations are given in Table 1. The experimental boundary conditions were used. A constant surface transfer coefficient is used in the calculations (β_v =0.01 m/s).

11. Result

The present study begins with a basic theory for anisotropic moisture flow in wood using Kirchhoff potentials. Based on the theory a calculation model and a computer program are developed. To test the model, material data from measurements are used in calculations of two-dimensional drying of a piece of wood. The calculated result is compared with measured ones in Fig. 7.. The calculated values are the ones in bold face. The result is given in moisture content mass by mass (kg/kg), in percent, at four different times during the drying process. The measured values are mean values for the weighed cubes and the calculated values are mean values for the corresponding calculation cell in the numerical mesh.

23	**22**	**23**	**20**	**21**	**22**	**22**	**22**	**22**	**21**	**21**	**21**	**16**
23	22	23	20	21	22	22	22	22	21	21	21	16
27	**29**	**28**	**28**	**29**	**29**	**30**	**30**	**29**	**27**	**28**	**25**	**18**
27	29	28	28	29	29	30	30	29	27	28	25	18
27	**31**	**30**	**32**	**32**	**31**	**32**	**34**	**31**	**31**	**30**	**28**	**20**
27	31	30	32	32	31	32	34	31	31	30	28	**20**
26	**28**	**29**	**30**	**31**	**30**	**29**	**33**	**30**	**28**	**29**	**27**	**19**
26	28	29	30	31	30	29	33	30	28	29	27	19
21	**24**	**22**	**23**	**23**	**24**	**23**	**22**	**21**	**22**	**21**	**21**	**16**
21	24	22	23	23	24	23	22	21	22	21	21	16

Time = 0 hours

13	**14**	**15**	**15**	**15**	**15**	**15**	**15**	**15**	**16**	**13**	**13**	**12**
13	14	14	13	15	15	15	15	16	16	15	15	13
14	**18**	**21**	**21**	**22**	**22**	**22**	**22**	**22**	**22**	**22**	**16**	**13**
14	19	20	21	20	20	20	20	20	21	20	18	15
15	**20**	**22**	**23**	**24**	**24**	**24**	**24**	**23**	**23**	**23**	**17**	**14**
15	20	22	23	21	22	22	22	23	21	20	19	15
14	**18**	**20**	**22**	**22**	**22**	**22**	**22**	**22**	**21**	**20**	**19**	**13**
15	20	22	23	19	21	20	20	22	20	19	18	15
12	**14**	**14**	**14**	**14**	**14**	**14**	**14**	**14**	**14**	**14**	**14**	**12**
12	15	16	15	15	17	14	15	15	16	15	13	12

Time = 72 hours

14	**16**	**17**	**17**	**17**	**17**	**17**	**17**	**17**	**17**	**15**	**15**	**13**
15	16	17	18	17	18	-	18	17	18	19	16	14
17	**23**	**24**	**25**	**25**	**25**	**26**	**26**	**25**	**25**	**26**	**19**	**15**
18	22	22	25	24	29	-	27	25	26	24	24	15
18	**24**	**27**	**27**	**27**	**28**	**28**	**28**	**27**	**27**	**26**	**21**	**16**
18	23	27	27	27	27	-	27	27	26	26	25	**18**
17	**23**	**25**	**25**	**26**	**26**	**26**	**26**	**25**	**25**	**24**	**22**	**15**
16	21	24	23	26	24	-	25	24	24	25	22	17
14	**16**	**17**	**17**	**17**	**18**	**17**	**17**	**17**	**17**	**17**	**16**	**13**
14	14	16	16	16	15	-	16	18	17	16	16	14

Time = 24 hours

9	**11**	**11**	**11**	**11**	**11**	**11**	**11**	**12**	**11**	**9**	**9**	**8**
10	11	12	12	12	13	-	12	12	12	14	12	9
11	**12**	**14**	**15**	**15**	**15**	**15**	**15**	**15**	**15**	**16**	**12**	**9**
12	12	15	15	14	15	-	14	15	16	16	14	12
11	**13**	**15**	**16**	**16**	**16**	**17**	**17**	**16**	**16**	**16**	**12**	**9**
12	14	15	15	15	16	-	16	16	16	18	16	12
11	**12**	**14**	**15**	**15**	**15**	**15**	**15**	**15**	**15**	**15**	**14**	**9**
12	13	13	15	16	15	-	16	16	15	16	15	12
10	**11**	**11**	**11**	**11**	**12**	**12**	**12**	**12**	**12**	**12**	**12**	**9**
-	10	10	12	11	12	-	12	13	11	13	12	10

Time = 144 hours

Figure 7. Comparison between calculated (top line, bold face) and measured (second line) moisture content at different time during drying

12. Discussion

The presented model gives the mathematical base for moisture flow calculations in wood. If the total air pressure and the temperature are constant the moisture state is determined by a single moisture state variable. The choice of potential does not really matter. Treated in a correct way, the result must be the same independently of the choice of potential. However, the use of different potentials may differ in simplicity to use mathematically and in numerical models. The use of Kirchhoff potential has distinct advantages in both those matters. In the moisture flow equation the functional-dependent flow coefficients vanishes. Only the difference in Kirchhoff potential determines the moisture flow. This will considerably simplify the implementation of the described theory into a numerical model.

Moisture flow coefficients must be determined from measurements. The use of Kirchhoff potentials has distinct advantages here too. An example is the above evaluation from steady-state measurements over a slab of the material. In a traditional evaluation, the derivative of $u(x)$ is used to determine $D_u(u)$. Then the integral of $D_u(u)$, (5), is used to determine the flow in the numerical model. This 'going in a circle' is not necessary when Kirchhoff potentials are used throughout the whole process, from measurements through mathematical and numerical modelling to moisture flow calculations.

The situation is more complicated at internal and external boundaries. Here, it is not sufficient to know $u(\psi)$. We have to go back to continuous variables such as relative humidity, vapour pressure etc. to solve the boundary flow balance. But it should be noted that the simplest way to deal with the flow in the material layers adjacent to the boundary surface is to use Kirchhoff potentials.

The calculated results show good agreement with the measured ones throughout the whole simulation time with one exception. The largest difference occurs in a cell after 24 hours. The measured value is 24% and the calculated is 19%. The cell with the largest discrepancy lies close to the boundary between sapwood and heartwood. In the beginning of the calculation, parts of the wood have moisture content above the fibre saturation point. This indicates uncertainties considering the moisture flow above fibre saturation.

The calculated values close to the outer boundary agrees well with the measured ones. The used value of β_v (0.01 m/s) to simulate the boundary transfer seems to be quite right.

The agreement is quite satisfactory considering the natural variation in wood from one piece to another. The model simulates well the asymmetric drying caused by the polar anisotropy and the non-linear moisture flow in both sapwood and heartwood.

It is also to be noticed that the computer calculation time is very short, although complications such as anisotropy and moisture-dependent moisture flow are taken into account in the model. A reason for this is the use of Kirchhoff potentials. By using them it is not necessary to evaluate integrals in each calculation step to obtain the moisture flow. The Kirchhoff potentials simplify the whole process from measurement, through mathematical and numerical modelling to numerical calculations.

References

Arfvidsson, J. and J. Claesson. 1989. A PC based Method to Calculate Moisture Transport. International Symposium, ICHMT, International centre for Heat and Mass Transfer. Dubrovnik, Yugoslavia.

Avramidis, S., Englezos, P., and Papathanasiou, T. 1992. Dynamic nonisothermal transport in hygroscopic porous media: moisture diffusion in wood. AIhE J.38(8): 1279-1287.

Carslaw, H. and J.C. Jaeger, 1959. Conduction of Heat in Solids, pp. 8-13, 2:nd ed., Oxford University Press, Oxford.

Claesson , J. 1993. A Few Remarks on Moisture Flow Potentials. International Energy Agency, Heat, Air and Moisture Transfer in Insulated Envelope Parts, Report Annex 24, Task 1, modelling.

Claesson, J. 1997. Mathematical Modelling of Moisture Transport. International Conference of COST Action E8 Wood Mechanics, Wood.water relations. Copenhagen, Denmark.

Lindgren, O. 1988. Non-destructive Measurements of Density and Moisture Content in Wood using Computed Tomography. Licentiate thesis. Royal Institure of Technology, Sweden.

Lindgren, O. 1992. medical CT-scannners for Non-destructive Wood Density and Moisture Content Measurements. Doctoral Thesis. Luleå University of Technology, Sweden.

Liu, J.Y. 1990. Lumber Drying in Medium with Variable Potentials. *In*: General papers: Phase change and convective heat transfer. Proceedings of AIAA/ASME thermophysics and heat transfer conference, Seattle, WA. Eds. K. Vafai, M Ebadian and T.Biller. The American Society of Mechanical Engeneers, New York. pp. 149-156.

Luikov, A.V,1966. Heat and Mass Transfer in Capillary-porous bodies. Pergamon Press, Oxford.

Plumb, O.A., C.A. Brown, and B.A. Olstead. 1984. Experimental Measurements of Heat and Mass Transfer During Convective Drying of Southern Pine. Wood Sci. Technol. 18: 187-204.

Rosenkilde, A. and J. Arfvidsson, 1997. Measurement and Evaluation of Moisture Transport Coefficients During Drying of Wood. Holzforschung 51: 372-380.

Samuelsson, A and J. Arfvidsson, 1994. Measurement and Calculation of Moisture Content Distribution During drying. Fourth International IUFRO Wood Drying Conference, Rotorua, New Zealand, August 9-13: 107-113.

Samuelsson, A. and O. Söderström. 1994. Measurement of Surface Emission Factors in Wood Drying. Fourth International IUFRO Wood Drying Conference, Rotorua, New Zealand, August 9-13: 107-113.

Stanish, M.A., G.S. Schajer, and F. Kayihan. 1986. A mathematical model of drying for hygroscopic porous media. AIChE J. 32(8): 1301-1311.